Bistability in a four-level laser with a resonant pump mode

T. C. Ralph
Department of Physics and Theoretical Physics, Australian National University, Canberra, Australian Capital Territory 2601, Australia
(Received 11 October 1993)

We investigate an optically pumped four-level laser in which both the laser and the pump form resonant cavity modes. We find that the system can exhibit absorptive bistability under conditions typical of solid-state lasers. Under conditions of high pump-cavity finesse, a bistability exists between below-threshold operation and maximum laser output.

PACS number(s): 42.65.Pc

I. INTRODUCTION

In recent years there has been much interest in the behavior of lasers under conditions where the dynamics of atomic levels other than the lasing levels need to be explicitly retained [1]. Interesting nonlinear behavior has been predicted, in particular in class-3 lasers, e.g., solid-state lasers. Given the rising importance of photonics in communications and measurement such research has technological as well as scientific significance.

Bistable output intensity has previously been predicted and demonstrated in lasers containing intracavity saturable absorbers [2,3]. At certain pump powers, two stable situations are possible: one in which the absorber atoms are unsaturated and quench lasing action, the other in which the absorber atoms are saturated and hence transparent. It has also been shown theoretically that bistability occurs in a three-level Raman laser when a resonant pump mode is created [4]. In this paper we predict that bistability can also occur in a four-level laser with homogeneously broadened pump and laser transitions typical of solid-state lasers.

We examine an optically pumped four-level laser in which both the pump and the laser form resonant cavity modes. Under certain conditions the pump mode can exhibit an absorptive bistability. This in turn results in bistable laser output. The lower branch of the laser output corresponds to the pump transition being unsaturated and is similar to that expected from a weakly depleted classical pump. The upper branch corresponds to saturation of the pump transition, i.e., maximum laser output. The width of the bistable region can be controlled by adjusting the finesse of the pump cavity and the energy level decay rates of the active atoms. Under conditions of high pump-cavity finesse the lower branch is below threshold while the upper branch is at maximum output power.

In the second section of this paper we will set up the model and derive the steady-state semiclassical results. In the third section we will examine the behavior of the laser threshold as a function of the pump-cavity decay rate. In the fourth section the bistable region will be examined. Bistability curves for the laser and conditions under which bistability appears will be presented. We demonstrate the feasibility of observing bistability with parameters typical of solid-state lasers.

II. THE LASER MODEL

Figure 1(a) is a schematic representation of a possible experimental setup. The atomic level scheme of the active atoms is depicted in Fig. 1(b). Our model consists of N of these four-level atoms interacting with an optical ring cavity mode via the resonant Jaynes-Cummings Hamiltonian

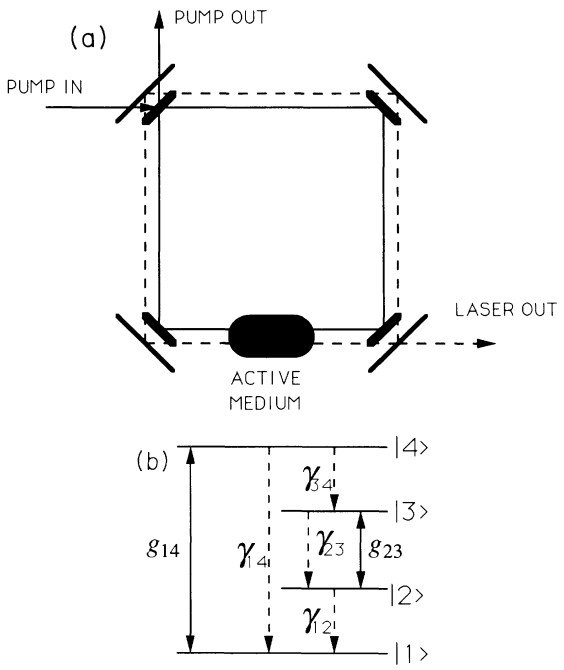

FIG. 1. (a) Schematic diagram of experimental realization of a four-level laser with quantized pump mode. The pump cavity is resonant with the pump transition of the atoms. The ratio of pump out to pump in (P_{out}/P_{in}) is determined by the reflectivity of the pump input mirror and the absorption of the active medium. (b) Energy level diagram for the lasing atoms.

$$\hat{H}_{23}=i\hbar g_{23}\sum_{\mu=1}^{N}(\hat{a}^{\dagger}\hat{\sigma}_{23\mu}^{-}-\hat{a}\hat{\sigma}_{23\mu}^{+}) , \tag{1}$$

where carets indicate operators, g_{ij} is the dipole coupling strength between the $|i\rangle$ to $|j\rangle$ level transition of an atom and the cavity, μ labels the different atoms, $\hat{a}$ and $\hat{a}^{\dagger}$ are the cavity mode annihilation and creation operators, and $\hat{\sigma}_{ij\mu}^{-}$ and $\hat{\sigma}_{ij\mu}^{+}$ are the Hermitian conjugate lowering and raising operators between levels $|i\rangle$ and $|j\rangle$ for the μth atom. The field phase factors have been absorbed into the definition of the atomic operators. In addition the atoms interact with a second optical cavity "pump" mode via the resonant Jaynes-Cummings Hamiltonian

$$\hat{H}_{14}=i\hbar g_{14}\sum_{\mu=1}^{N}(\hat{b}^{\dagger}\hat{\sigma}_{14\mu}^{-}-\hat{b}\hat{\sigma}_{14\mu}^{+}) , \tag{2}$$

where $\hat{b}$ and $\hat{b}^{\dagger}$ are the pump mode annihilation and creation operators. The pump mode is driven by a close-to-resonance field interacting with the cavity via the Hamiltonian

$$\hat{H}_{C}=i\hbar\sqrt{2\kappa_b}(Ee^{-i\omega_p t}\hat{b}^{\dagger}-E^{*}e^{i\omega_p t}\hat{b}) . \tag{3}$$

The photon flux of the incident field is given by EE^{*}. The frequency of the incident field is ω_p. The pump-cavity damping rate due to the input-output mirror is $2\kappa_b$. Following standard techniques [5,6] we couple the atoms and cavity to reservoirs and derive a master equation for the reduced density operator $\hat{\rho}$ of the atoms and cavity. Included in our laser model are atomic spontaneous emissions from level $|4\rangle$ to level $|3\rangle$, from level $|3\rangle$ to level $|2\rangle$, from level $|2\rangle$ to level $|1\rangle$, and from level $|4\rangle$ to level $|1\rangle$, at rates γ_{34}, γ_{23}, γ_{12}, and γ_{14}, respectively. γ_{p1} is the rate of collisional or lattice induced phase decay of the lasing coherence while γ_{p2} is the rate of collisional or lattice induced phase decay of the pump coherence. The laser cavity damping rate is $2\kappa_a$. The resulting interaction-picture master equation is

$$\frac{\partial}{\partial t}\hat{\rho}=\frac{1}{i\hbar}[\hat{H}_{23},\hat{\rho}]+\frac{1}{i\hbar}[\hat{H}_{14},\hat{\rho}]+\frac{1}{i\hbar}[\hat{H}_{C},\hat{\rho}]+\tfrac{1}{2}(\gamma_{14}L_{14}+\gamma_{34}L_{34}+\gamma_{12}L_{12}+\gamma_{23}L_{23})\hat{\rho}$$

$$+\tfrac{1}{4}(\gamma_{p1}L_{3-2}+\gamma_{p2}L_{4-1})\hat{\rho}+\kappa_a(2\hat{a}\hat{\rho}\hat{a}^{\dagger}-\hat{a}^{\dagger}\hat{a}\hat{\rho}-\hat{\rho}\hat{a}^{\dagger}\hat{a})+\kappa_b(2\hat{b}\rho\hat{b}^{\dagger}-\hat{b}^{\dagger}\hat{b}\rho-\rho\hat{b}^{\dagger}\hat{b}) , \tag{4}$$

with

$$L_{ij}\hat{\rho}=\sum_{\mu=1}^{N}(2\hat{\sigma}_{ij\mu}^{-}\hat{\rho}\hat{\sigma}_{ij\mu}^{+}-\hat{\sigma}_{ij\mu}^{+}\sigma_{ij\mu}^{-}\hat{\rho}-\hat{\rho}\hat{\sigma}_{ij\mu}^{+}\hat{\sigma}_{ij\mu}^{-}) ,$$

$$L_{ij}^{\dagger}\hat{\rho}=\sum_{\mu=1}^{N}(2\hat{\sigma}_{ij\mu}^{+}\hat{\rho}\hat{\sigma}_{ij\mu}^{-}-\hat{\sigma}_{ij\mu}^{-}\hat{\sigma}_{ij\mu}^{+}\hat{\rho}-\hat{\rho}\hat{\sigma}_{ij\mu}^{-}\hat{\sigma}_{ij\mu}^{+}) ,$$

$$L_{i-j}\hat{\rho}=\sum_{\mu=1}^{N}(2(\hat{\sigma}_{i\mu}-\hat{\sigma}_{j\mu})\hat{\rho}(\hat{\sigma}_{i\mu}-\hat{\sigma}_{j\mu})$$

$$-(\hat{\sigma}_{i\mu}-\hat{\sigma}_{j\mu})^{2}\hat{\rho}-\hat{\rho}(\hat{\sigma}_{i\mu}-\hat{\sigma}_{j\mu})^{2}) .$$

The interaction Hamiltonians are obtained using electric dipole and rotating wave approximations. These are good approximations at optical frequencies. The finesse of the cavity is assumed to be sufficiently high that one may make the mean-field approximation. Other major simplifying assumptions contained in these models of the laser are (i) single-mode operation, (ii) plane-wave approximation, and (iii) constant number of atoms.

The semiclassical equations of motion for the operator expectation values may be obtained directly from the master equation by making the approximation of factorizing expectation values. This corresponds physically to ignoring the quantum fluctuations in the field. We obtain the following equations of motion (and their complex conjugates):

$$\begin{aligned}
&\dot{\tilde{\alpha}}=\tilde{g}_{23}\tilde{J}_{23}-\kappa_a\tilde{\alpha} , \quad \dot{\tilde{\beta}}=\tilde{g}_{14}\tilde{J}_{14}-(\kappa_b+i\Delta\omega)\tilde{\beta}+\sqrt{2\kappa_b}\tilde{E} ,\\
&\dot{\tilde{J}}_{14}=\tilde{g}_{14}(\tilde{J}_4-\tilde{J}_1)\tilde{\beta}-\tfrac{1}{2}(\gamma_{34}+\gamma_{14}+2\gamma_{p2})\tilde{J}_{14} ,\\
&\dot{\tilde{J}}_{23}=\tilde{g}_{23}(\tilde{J}_3-\tilde{J}_2)\tilde{\alpha}-\tfrac{1}{2}(\gamma_{23}+\gamma_{12}+2\gamma_{p1})\tilde{J}_{23} ,\\
&\dot{\tilde{J}}_{2}=\tilde{g}_{23}(\tilde{J}_{23}\tilde{\alpha}^{\dagger}+\tilde{J}_{23}^{+}\tilde{\alpha})+\gamma_{23}\tilde{J}_3-\gamma_{12}\tilde{J}_2 ,\\
&\dot{\tilde{J}}_{3}=-\tilde{g}_{23}(\tilde{J}_{23}\tilde{\alpha}^{\dagger}+\tilde{J}_{23}^{+}\tilde{\alpha})+\gamma_{34}\tilde{J}_4-\gamma_{23}\tilde{J}_3 ,\\
&\dot{\tilde{J}}_{4}=-\tilde{g}_{14}(\tilde{J}_{14}\tilde{\beta}^{\dagger}+\tilde{J}_{14}^{+}\tilde{\beta})-(\gamma_{34}+\gamma_{14})\tilde{J}_4 ,
\end{aligned} \tag{5}$$

where $\Delta\omega=\omega_p-\omega_c$ is the detuning of the pump from the cavity resonance (ω_c) and

$$\alpha^{\dagger}=\langle\hat{a}^{\dagger}\rangle , \quad \beta^{\dagger}=\langle\hat{b}^{\dagger}\rangle ,$$

$$\alpha=\langle\hat{a}\rangle , \quad \beta=\langle\hat{b}\rangle ,$$

$$J_{ij}^{+}=\langle\hat{J}_{ij}^{-}\rangle\equiv\sum_{\mu=1}^{N}\langle\hat{\sigma}_{ij\mu}^{+}\rangle ,$$

$$J_i=\langle\hat{J}_i\rangle\equiv\sum_{\mu=1}^{N}\langle\hat{\sigma}_{i\mu}\rangle ,$$

$$J_{ij}=\langle\hat{J}_{ij}\rangle\equiv\sum_{\mu=1}^{N}\langle\hat{\sigma}_{ij\mu}^{-}\rangle$$

are the expectation values of the corresponding operators. J_i is the expectation value of the collective population operator for the ith level. The tilde indicates the fol-

lowing scaling with atomic number, N:

$$\alpha=\tilde{\alpha}N^{1/2}\ ,\quad \beta=\tilde{\beta}N^{1/2}\ ,\quad J_{ij}=\tilde{J}_{ij}N\ ,$$
$$J_i=\tilde{J}_iN\ ,\quad g=\tilde{g}N^{-1/2}\ ,\quad E=\tilde{E}N^{1/2}\ .$$

These equations may be solved in the steady state for the amplitude squared, $|\tilde{\alpha}|^2$, which is approximately equal to $\tilde{n}\equiv$ number of laser photons per atom in the cavity (N.B., from this point on we use $\tilde{\alpha}$ and $\tilde{\beta}$ to represent the steady-state values of the laser and pump mode amplitudes).

The phase of $\tilde{\alpha}$ is undetermined, hence $\tilde{\alpha}$ can be chosen to be real without lack of generality. The phase of $\tilde{\beta}$ is determined by the phase of the driving field, $\tilde{E}$. By choosing the arbitrary phase of the driving field to be such that

$$\tilde{E}=\tilde{E}_r+i\frac{\Delta\omega}{\sqrt{2\kappa_b}}\tilde{\beta}_r\ , \tag{6}$$

where $\tilde{E}_r$ is the real part of the driving field and $\tilde{\beta}_r$ is the steady-state solution for the real part of the pump mode amplitude, we ensure that the imaginary part of $\tilde{\beta}$ is zero, i.e., the physical solution(s) for $\tilde{\beta}$ will be real ($\tilde{\beta}_r=\tilde{\beta}$). This significantly simplifies the calculations. We emphasize that this choice of the driving field phase [Eq. (6)] is not a special condition. In the absence of a reference phase the absolute phase of the driving field has no physical significance, hence our solutions are quite general.

The pump mode amplitude is then given by the following cubic equation:

$$\frac{4\tilde{g}_{14}\kappa_b}{\gamma_2\gamma_{12}}\left[\frac{\gamma_{12}+\gamma_{34}}{\gamma_{14}+\gamma_{34}}\right]\tilde{\beta}^3-\frac{4\tilde{g}_{14}\sqrt{2\kappa_b}\tilde{E}_r}{\gamma_2\gamma_{12}}\left[\frac{\gamma_{12}+\gamma_{34}}{\gamma_{14}+\gamma_{34}}\right]\tilde{\beta}^2$$
$$+\left[\frac{\kappa_b}{\tilde{g}_{14}}-\frac{\kappa_b\tilde{g}_{14}\gamma_1}{\tilde{g}_{23}^2\gamma_2}+\frac{\tilde{g}_{14}}{\gamma_2}\right]\tilde{\beta}-\frac{\sqrt{2\kappa_b}\tilde{E}_r}{\tilde{g}_{14}}=0\ , \tag{7}$$

with

$$\gamma_1=\frac{\gamma_{23}}{2}+\frac{\gamma_{12}}{2}+\gamma_{p1}\ ,$$
$$\gamma_2=\frac{\gamma_{34}}{2}+\frac{\gamma_{14}}{2}+\gamma_{p2}\ .$$

The laser mode photon number is then either $\tilde{n}=0$ or

$$\tilde{n}=\frac{\sqrt{2\kappa_b}\tilde{E}_r}{\kappa_a}\left[1-\frac{\gamma_{23}}{\gamma_{12}}\right]\left[\frac{\gamma_{34}}{\gamma_{14}+\gamma_{34}}\right]\tilde{\beta}-\frac{\kappa_b}{\kappa_a}$$
$$\times\left[1-\frac{\gamma_{23}}{\gamma_{12}}\right]\left[\frac{\gamma_{34}}{\gamma_{14}+\gamma_{34}}\right]\tilde{\beta}^2-\frac{\gamma_{23}\gamma_1}{2\tilde{g}_{23}^2}\ . \tag{8}$$

The steady-state solutions for the populations and polarizations are given by

$$\tilde{J}_4=\frac{2}{\gamma_{34}}\left[\sqrt{2\kappa_b}\tilde{E}_r\tilde{\beta}-\kappa_b\tilde{\beta}^2\right]\ ,$$
$$\tilde{J}_2=\frac{2}{\gamma_{12}}\left[\sqrt{2\kappa_b}\tilde{E}_r\tilde{\beta}-\kappa_b\tilde{\beta}^2\right]\ ,$$
$$\tilde{J}_3=\frac{2}{\gamma_{23}}(\sqrt{2\kappa_b}\tilde{E}_r\tilde{\beta}-\kappa_b\tilde{\beta}^2-\kappa_a\tilde{n})\ ,$$
$$\tilde{J}_1=1-\tilde{J}_2-\tilde{J}_3-\tilde{J}_4\ , \tag{9}$$
$$\tilde{J}_{14}=\frac{\kappa_b}{\tilde{g}_{14}}\tilde{\beta}-\frac{\sqrt{2\kappa_b}\tilde{E}_r}{\tilde{g}_{14}}\ ,$$
$$\tilde{J}_{23}=\frac{\kappa_a}{\tilde{g}_{23}}\tilde{\alpha}\ .$$

As Eq. (7) has in general three solutions so there are in general four solutions for $\tilde{n}$. In the following sections we consider the behavior of the solutions as a function of the pump-cavity decay rate ($2\kappa_b$) using linear stability analysis to identify the stable solution(s). The stability analysis is carried out in the standard way be examining the eigenvalues of the linearized drift matrix defined by

$$A_{\xi,\xi;0}=-\frac{\partial}{\partial\tilde{\alpha}_\xi}\dot{\tilde{\alpha}}_\xi\Big|_{\tilde{\alpha}=\tilde{\alpha}_0}\ ,$$
$$\tilde{\alpha}=(\tilde{\alpha},\tilde{\alpha}^\dagger,\tilde{\beta},\tilde{\beta}^\dagger,\tilde{J}_{14},\tilde{J}_{23},\tilde{J}_2,\tilde{J}_3,\tilde{J}_4,\tilde{J}_{23}^+,\tilde{J}_{14}^+)\ ,$$

where $\dot{\tilde{\alpha}}_\xi$ is the right-hand side of the corresponding Eq. (5) and we have used the subscript 0 to emphasize that the steady-state values of the variables are substituted into the matrix. A particular solution of Eq. (8) is stable if the real parts of the eigenvalues of the drift matrix are all positive.

III. THRESHOLD BEHAVIOR

When the pump-cavity decay rate is rapid the laser behaves in the usual way. Equation (7) only ever has one real solution and hence so does Eq. (8). At low pump powers Eq. (8) is negative and unstable, while the zero solution is stable, i.e., the laser is below threshold. As the pump power is increased Eq. (8) becomes positive and stable, while the zero solution becomes unstable, i.e, the laser is above threshold. The laser output then increases linearly with pump power until the pump transition saturates at high pump powers [see Fig. 2(a)].

If the lasing transition is strongly coupled to the laser cavity ($\tilde{g}_{23}^2/\gamma_1\kappa_a\gg1$) then threshold will occur at sufficiently low pump powers such that $\tilde{\beta}\ll1$. Hence Eq. (7) can be simplified by dropping all but the linear term in $\tilde{\beta}$. Using this approximation and the strong coupling condition to substitute into Eq. (8) we obtain the following threshold condition for the real part of the driving field:

$$\tilde{E}_{rt}^2=\frac{\gamma_{23}\gamma_1\gamma_2\kappa_a}{4\tilde{g}_{23}^2\tilde{g}_{14}^2\kappa_b}\left[\kappa_b+\frac{\tilde{g}_{14}^2}{\gamma_2}\right]^2\frac{(\gamma_{14}+\gamma_{34})}{\gamma_{34}}\ , \tag{10}$$

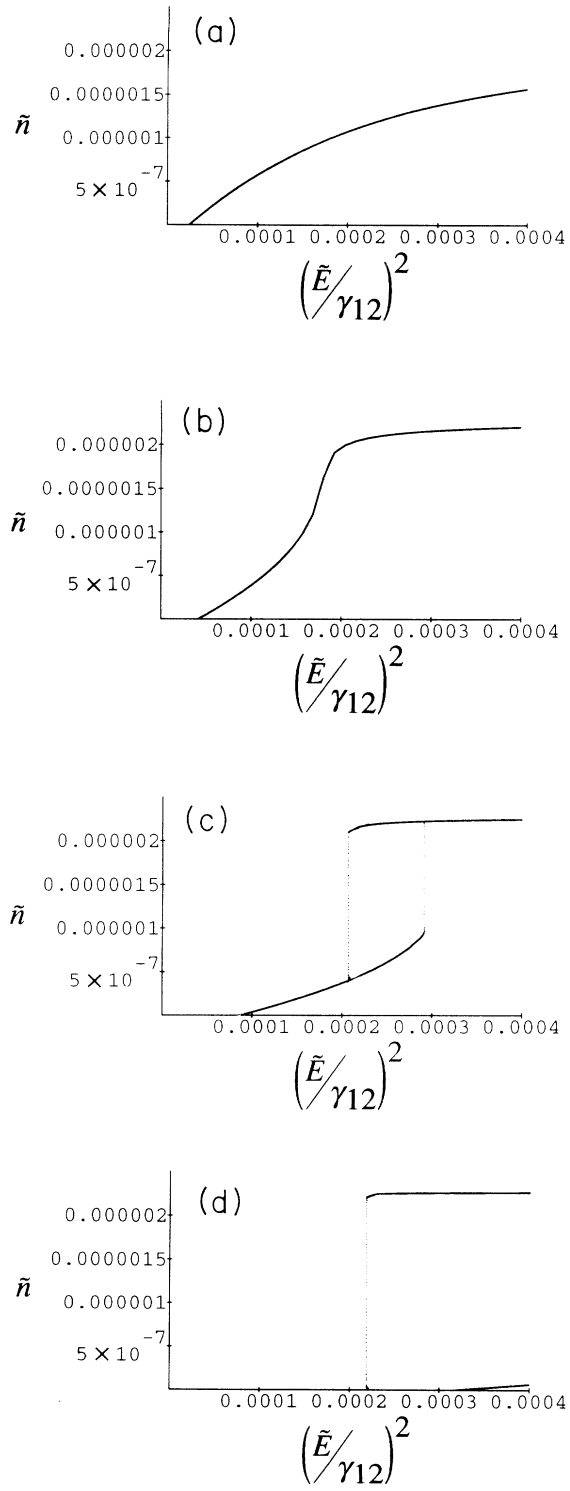

FIG. 2. Intracavity laser photons per atom ($\tilde{n}$) versus driving field photon flux per atom [$(\tilde{E}/\gamma_{12})^2$], in units of γ_{12}, for a resonant driving field ($\Delta\omega=0$). Only the stable solutions are shown. In (a) we see normal laser behavior, $\kappa_b=150\gamma_{12}$ s^{-1}. In (b) we see nonlinear behavior emerging; $\kappa_b=10\gamma_{12}$ s^{-1}. In (c) we see bistable behavior; $\kappa_b=4\gamma_{12}$ s^{-1}. Finally in (d) we see bistability between below threshold and maximum laser output; $\kappa_b=\gamma_{12}$ s^{-1}. Other parameters in units of γ_{12} are $\tilde{g}_{14}=\tilde{g}_{23}=3\times10^4$, $\gamma_1=\gamma_2=8\times10^6$, $\gamma_{34}=7.5\times10^{-4}$, $\gamma_{14}=0$, $\gamma_{23}=0.5\times10^{-4}$, and $\kappa_a=45$.

where we have also assumed that $\gamma_{23}\ll\gamma_{12}$. As the pump-cavity decay rate is made slower the laser threshold moves to lower incident powers. A minimum value of

$$\tilde{E}^2_{rt\min}=\frac{\gamma_{23}\gamma_1\kappa_a}{\tilde{g}^2_{23}}\frac{(\gamma_{14}+\gamma_{34})}{\gamma_{34}} \tag{11}$$

is reached when

$$\kappa_b=\frac{\tilde{g}^2_{14}}{\gamma_2}\ .$$

Decay rates slower than $\tilde{g}^2_{14}/\gamma_2$ lead to higher threshold powers. This behavior can be understood in terms of the absorption characteristics of the pump cavity. For an on-resonance driving field the output pump power ($P_{\rm out}$) can be related to the input pump power ($P_{\rm in}$) by [7]

$$\frac{P_{\rm out}}{P_{\rm in}}=\frac{1}{R}\left[\frac{R-\sqrt{R}\,(1-\varepsilon)}{1-\sqrt{R}\,(1-\varepsilon)}\right]^2, \tag{12}$$

where R is the intensity reflectivity of the input-output mirror and ε is the single-pass intensity-loss coefficient. In the good-cavity limit ($2\kappa_b L/c\ll1$, where L is the cavity length and c is the speed of light) this expression is approximately

$$\frac{P_{\rm out}}{P_{\rm in}}\cong1-\frac{4\kappa_b\gamma_{ab}}{(\kappa_b+\gamma_{ab})}\ , \tag{13}$$

where γ_{ab} is the rate at which photons are absorbed by the active medium. From the semiclassical equations [Eq. (5)] we get

$$\gamma_{ab}=-\frac{\tilde{g}_{14}\tilde{J}_{14}}{\tilde{\beta}}\ . \tag{14}$$

Hence Eqs. (13) and (14) give the extent to which the pump mode is absorbed for particular parameters and pump rate. In the limit of low pump powers the approximation used to obtain Eq. (10) can be used to simplify Eq. (13). We obtain

$$\frac{P_{\rm out}}{P_{\rm in}}\cong\left[1-\frac{2\kappa_b}{\kappa_b+\dfrac{g^2_{14}}{\gamma_2}}\right]^2. \tag{15}$$

Equation (15) has a minimum of zero when $\kappa_b=g^2_{14}/\gamma_2$. This represents complete absorption of the pump (the pump is impedance matched to the cavity) and produces the minimum threshold power. At both higher and lower values of the pump-cavity decay rate absorption is incomplete at low pump powers.

IV. BISTABILITY

When $\kappa_b<g^2_{14}/\gamma_2$ complete absorption of the pump occurs at higher pump powers. If we set Eq. (13) to zero (i.e., complete absorption of the pump) and use the steady-state semiclassical equations to solve for $\tilde{E}_r$ we obtain

$$\tilde{E}_{r0}^2=\frac{\gamma_{12}\left[1-\frac{\gamma_1\kappa_a}{\tilde{g}_{23}^2}-\frac{\gamma_2\kappa_b}{\tilde{g}_{14}^2}\right]}{2\left[\frac{\gamma_{12}+\gamma_{34}}{\gamma_{14}+\gamma_{34}}\right]} . \tag{16}$$

The increased absorption at higher pump powers produces a nonlinear relationship between pump and output power below saturation [see Fig. 2(b)]. As we continue to reduce κ_b, $\tilde{E}_{r0}^2$ reaches a maximum value then begins to fall again.

When the pump decay rate has been made sufficiently small Eq. (7), and hence Eq. (8), has three real solutions for a range of pump powers. Linear stability analysis reveals that two of these solutions are stable, indicating bistability [see Fig. 2(c)]. Using standard techniques for the solution of cubic equations we find that Eq. (7) has three real solutions for the following range of the real part of the driving field (where the positive sign gives the upper limit and the negative sign gives the lower limit):

$$\tilde{E}_{r\pm}^2=\frac{\tilde{g}_{23}^4\tilde{g}_{14}^4+20\tilde{g}_{23}^4\tilde{g}_{14}^2\gamma_2\kappa_b-8\tilde{g}_{23}^4\gamma_2^2\kappa_b^2-2\tilde{g}_{23}^2\tilde{g}_{14}^4\gamma_1\kappa_a-20\tilde{g}_{23}^2\tilde{g}_{14}^2\gamma_2\gamma_1\kappa_a\kappa_b+\tilde{g}_{14}^4\gamma_1^2\kappa_a^2}{64\kappa_b\tilde{g}_{23}^4\gamma_2\tilde{g}_{14}^2\left[\frac{\gamma_{34}+\gamma_{12}}{\gamma_{12}(\gamma_{34}+\gamma_{14})}\right]}$$
$$\pm\frac{\tilde{g}_{14}\sqrt{\tilde{g}_{23}^2-\gamma_1\kappa_a}(\tilde{g}_{23}^2\tilde{g}_{14}^2-8\tilde{g}_{23}^2\gamma_2\kappa_b-\tilde{g}_{14}^2\gamma_1\kappa_a)^{3/2}}{64\kappa_b\tilde{g}_{23}^4\gamma_2\tilde{g}_{14}^2\left[\frac{\gamma_{34}+\gamma_{12}}{\gamma_{12}(\gamma_{34}+\gamma_{14})}\right]} . \tag{17}$$

The last line of Eq. (17) determines whether or not we are in the bistable regime. If the sum under the cubed square root is negative then $\tilde{E}_{r\pm}^2$ will be complex indicating that Eq. (7) has only one solution and the system has no bistability (note that the sum under the square root in the last line must always be positive otherwise lasing action cannot be initiated). Hence we have the following condition for bistability:

$$\frac{8\gamma_2\kappa_b}{\tilde{g}_{14}^2}+\frac{\gamma_1\kappa_a}{\tilde{g}_{23}^2}<1 . \tag{18}$$

Notice that unlike the three-level laser [4] bistability is not dependent on the ratio of longitudinal to transverse decay rates. If the bistability condition [Eq. (18)] is strongly satisfied a binomial expansion can be used to simplify Eq. (17). We obtain simpler expressions for $\tilde{E}_{r+}$ and $\tilde{E}_{r-}$, namely,

$$\tilde{E}_{r+}^2\cong\frac{2\tilde{g}_{23}^4\tilde{g}_{14}^4+8\tilde{g}_{23}^4\tilde{g}_{14}^2\gamma_2\kappa_b+16\tilde{g}_{23}^4\gamma_2^2\kappa_b^2-4\tilde{g}_{23}^2\tilde{g}_{14}^4\gamma_1\kappa_a-8\tilde{g}_{23}^2\tilde{g}_{14}^2\gamma_2\gamma_1\kappa_a\kappa_b+2\tilde{g}_{14}^4\gamma_1^2\kappa_a^2}{64\kappa_b\tilde{g}_{23}^4\gamma_2\tilde{g}_{14}^2\left[\frac{\gamma_{34}+\gamma_{12}}{\gamma_{12}(\gamma_{34}+\gamma_{14})}\right]}$$
$$\tilde{E}_{r-}^2\cong\frac{\gamma_{12}\left[1-\frac{\gamma_1\kappa_a}{\tilde{g}_{23}^2}-\frac{\gamma_2\kappa_b}{\tilde{g}_{14}^2}\right]}{2\left[\frac{\gamma_{12}+\gamma_{34}}{\gamma_{14}+\gamma_{34}}\right]} . \tag{19}$$

Notice that the expression for $\tilde{E}_{r-}$ is the same as Eq. (16), i.e., the lower limit of the upper branch of the bistability is given by the condition for total absorption of the pump mode. In the limit of Eq. (18) being very strongly satisfied Eqs. (19) reduce to

$$\tilde{E}_{r+}^2\approx\frac{\tilde{g}_{14}^2\gamma_{12}(\gamma_{34}+\gamma_{14})}{32\kappa_b\gamma_2(\gamma_{12}+\gamma_{34})} ,$$
$$\tilde{E}_{r-}^2\approx\frac{\gamma_{12}(\gamma_{34}+\gamma_{14})}{2(\gamma_{12}+\gamma_{34})} . \tag{20}$$

Notice that the lower limit of the bistable region is independent of the pump-cavity decay rate in this limit. However threshold power for the lower branch continues to rise with decreasing κ_b. Hence when κ_b is sufficiently small we encounter a situation in which the upper branch extends below the threshold of the lower branch establishing a bistability between the upper branch and the zero solution [see Fig. 2(d)]. Comparing $\tilde{E}_{r-}$ as given by Eq. (20) with the threshold condition [Eq. (10)] we obtain the following condition for the bistability to extend below threshold:

$$\kappa_b<\frac{\gamma_{23}\gamma_1\tilde{g}_{14}^2\kappa_a(\gamma_{34}+\gamma_{12})}{2\tilde{g}_{23}^2\gamma_2\gamma_{12}(\gamma_{34}+\gamma_{14})} . \tag{21}$$

Observing bistable behavior experimentally will rely on satisfying two requirements: (i) creating a sufficiently high-finesse pump cavity such that Eq. (18) is satisfied

and (ii) being able to reach the pump powers required by Eq. (17) to be within the bistable region. We now discuss these requirements. The pump absorption cross section (σ_p) is related to our parameters via

$$\frac{\tilde{g}_{14}^2}{\gamma_2}=\frac{c\sigma_p\rho}{4} . \tag{22}$$

Similarly the stimulated emission cross section (σ_s) is related by

$$\frac{\tilde{g}_{23}^2}{\gamma_1}=\frac{c\sigma_s\rho}{4} . \tag{23}$$

A reasonable value for these cross sections in solid-state materials is $\sigma_l=\sigma_p=5\times10^{-25}$ m^2. Taking $\rho=1\times10^{26}$ m^{-3} and $\kappa_a=200$ MHz we find minimum threshold power will be achieved for a pump cavity with $\kappa_b=2{,}500$ MHz and hence nonlinear behavior will emerge for slower pump-cavity decays. Bistability will occur when $\kappa_b<290$ MHz. These cavity linewidths are easily attained.

The powers required to reach the bistable region are determined by the decay rates of the active atoms. In many solid-state lasers these decay rates are millions per second. From Eq. (18) we see that similarly high pump rates and hence prohibitively high pump powers would then be required to reach the bistable region. However the decay rates of the active atoms can be affected by the host materials, e.g., decay rates of hundreds per second are common in fluoride glasses [8]. In such a host, a laser with a small cross-sectional area (e.g., a fiber laser) with a pump mode on resonance with the driving field, would require pump powers in the tens of milliwatts to reach the bistable region. For such a laser bistability between above- and below-threshold operation would occur when $\kappa_b<20$ MHz. The effect of the driving field being off resonance is to raise the pump power required to reach the bistable region in accordance with

$$|\tilde{E}|^2=\tilde{E}_r^2+\frac{\Delta\omega^2}{2\kappa_b}\tilde{\beta}^2 . \tag{24}$$

V. CONCLUSION

In this paper we have investigated the properties of an optically pumped four-level laser in which both the laser and the pump from resonant cavity modes. We have found that the absorption characteristics of the pump-cavity–active-medium system leads to interesting nonlinear behavior. In particular, bistable behavior is predicted when the finesse of the pump cavity is sufficiently high. Under conditions of very high pump-cavity finesse a bistability can exist between maximum laser output power and below-threshold operation. We have shown that for conditions typical of solid-state lasers bistability will occur for pump-cavity linewidths less than about 300 MHz. The pump power required to reach the bistable region depends strongly on the atomic decay rates of the active atoms.

ACKNOWLEDGMENTS

We acknowledge useful discussions with Craig Savage, Mathew Taubman, and Jim Cresser. This work was supported by the Australian Research Council.

[1] For example, T. C. Ralph and C. M. Savage, Phys. Rev. A **44**, 7809 (1991); H. Ritsch, M. A. M. Marte, and P. Zoller, Europhys. Lett. **19**, 7 (1992); T. C. Ralph, A. J. Stevenson, C. M. Savage, and H.-A. Bachor, Opt. Lett. **18**, 1162 (1993).

[2] L. A. Lugatio, P. Mandel, S. T. Dembinski, and A. Kossakowski, Phys. Rev. A **18**, 238 (1978).

[3] E. Arimondo and B. M. Dinelli, Opt. Commun. **44**, 277 (1983).

[4] W. Lu, J. S. Uppal, and R. G. Harrison, Opt. Commun. **74**, 393 (1990).

[5] W. H. Louisell, *Quantum Statistical Properties of Radiation* (Wiley, New York, 1973).

[6] H. Haken, *Laser Theory,* edited by S. Flugge, Encyclopedia of Physics Vol. XXX/2c (Springer-Verlag, Heidelberg, 1970).

[7] A. E. Siegman, *Lasers* (University Science Books, Mill Valley, 1986).

[8] D. C. Yeh, W. A. Sibley, M. Suscavage, and M. G. Drexhage, J. Appl. Phys. **62**, 266 (1987).

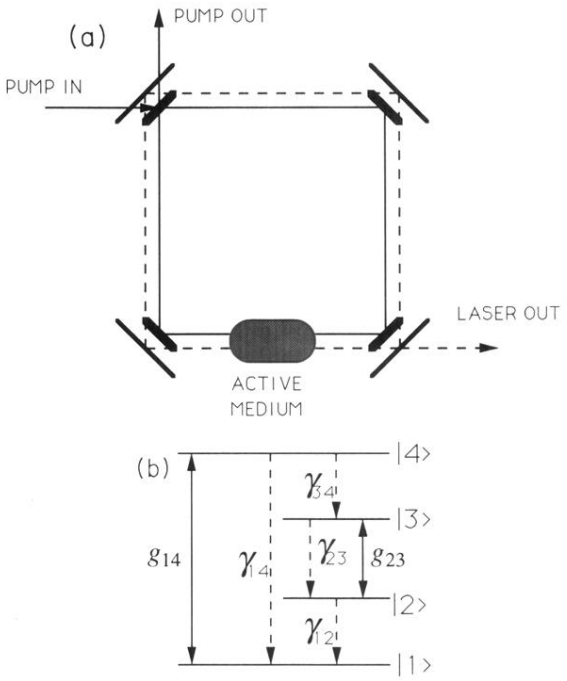

FIG. 1. (a) Schematic diagram of experimental realization of a four-level laser with quantized pump mode. The pump cavity is resonant with the pump transition of the atoms. The ratio of pump out to pump in ($P_{\text{out}}/P_{\text{in}}$) is determined by the reflectivity of the pump input mirror and the absorption of the active medium. (b) Energy level diagram for the lasing atoms.